Solid earth modulation of marine outlet glacier response

Andrew Hoffman[1]

[1]Department of Earth and Space Sciences, University of Washington, Seattle, Washington, USA

Correspondence: hoffmaao@uw.edu

Abstract. The dynamics of marine-terminating outlet glaciers and the solid earth are of fundamental interest in glaciology. In this study, we analyze the response of a coupled marine outlet glacier-bedrock system to different sources of climate forcing. We find that isostacy fundamentally changes the response of marine outlet glacier systems to surface-mass-balance forcing applied over the interior and the oceanic forcing applied at the grounding line. The reduced model is shown to emulate the behavior of more complex numerical models of ice flow. Together, these models demonstrate that ocean forcing first engages the fast, local response, and then the slow adjustment of interior ice, whereas surface-mass-balance forcing is dominated by the slow interior adjustment. We also demonstrate the importance of the timescales of stochastic forcing for assessing the natural variability of outlet glaciers, highlighting that decadal persistence in ocean variability can affect the behavior of outlet glaciers on centennial and longer timescales. Finally, we show that these transient responses have important implications for: attributing observed glacier changes to natural or anthropogenic influences; the future change already committed by past forcing; and the impact of past climate changes on the preindustrial glacier state, against which current and future anthropogenic influences are assessed.

1 Introduction

Ice-sheet mass change in Antarctica and Greenland is primarily controlled by two processes: thinning at the marine ice-sheet margin due to ocean melt and consequent grounding line position change, and changes in accumulation and surface melt in the ice-sheet interior. These mass change mechanisms affect the configuration of the ice sheet differently, eliciting different ice-sheet responses. Ocean melt forcing tends to evoke a rapid (multi-decadal) response in glacier length that drives inland thinning from the margin while surface mass balance forcing drives a slow (multi-century) response integrated over the time it takes for the glacier to convey the surface mass balance anomaly to the grounding line (Christian et al 2020, Robel et al 2018). These response times carry significance for the temporal controls on glacier behavior and can be related to properties of the conveying ice-stream like the glacier geometry, the mechanisms that govern glacier sliding, and the forcing variability. Marine ice-sheet response times also overlap with the characteristic viscoelastic response time of the solid earth. The interplay between the deforming geoid due to ice loading and unloading and glacier mass change has been well studied (i.e Weertman 1972; Weertman 1980b; Pollard et al. 1984) and tangentially linked to the stability of geometrically vulnerable marine outlet glaciers through local sea-level adjustment (Gomez et al 2010). Understanding the past and future contribution of ice-sheet mass change to distributed sea-level change has motivated acquisition of geodetic time series and coupled simulation of the

earth, ice-sheet, sea-level system. Together, observations and fully coupled global models have helped quantify committed spatial patterns of sea-level change and the imprinted signature of past ice-sheet configurations in paleo sea-level markers; however, fundamental questions remain regarding the coupled influence of forcing variability, and the natural frequencies of the solid-earth system on ice-sheet response.

Here we combine a simple kinematic description of a marine ice-sheet with a simplified model of the lithosphere to understand the response spectra of glacier volume and length change due to isostasy. Our approach is to conduct idealized model experiments that isolate key physical principles of coupled glacier solid-earth system in response to climate variability. We follow Robel et al (2018), and Christian et al. (2020) and focus exclusively on stable prograde geometries where the reduced model yields simple physical and mathematical interpretations of a more complicated numerical model's response to forcing.

We first review the problem and use a dynamical model to understand the filtering properties of a simple marine terminating outlet glacier-bedrock coupled system. We then build on simple kinematic models of marine outlet glacier dynamics, adding a glacier isostatic adjustment (GIA) stage and linearize the kinematic system of equations to understand the projection of surface mass balance and ocean melt forcing onto the eigenmodes of a model that includes the effects of GIA. We then use the modified glacier response spectra and the character of perturbations about stable solutions to understand the relative magnitude of GIA on ice sheet mass change. We show that the stable outlet glacier coupled to the deflectable lithosphere resonates at a frequency that depends on the response time of the asthenosphere as well as the geometry, rheology and sliding properties of the glacier.

2 Simple ice-sheet-bedrock model and response to ocean and interior forcing

Before describing the models we use to understand coupled ice-sheet-bedrock response to external forcing, it is useful to begin by describing the geometry and basic flux arguments of the system we are investigating. We consider an idealized stable outlet glacier resting on continental lithosphere, a schematic of which is presented in figure 1a. Ice enters as snow accumulates over the interior and flows from the interior towards the ocean on a prograde bed, exiting the system where it reaches floatation at the grounding zone. Beyond this point, floating ice is assumed to calve or melt due to contact with the ocean. The ice sheet rests on the lithosphere, which we assume to be in floating equilibrium with the underlying heavier substrate in the asthenosphere. As the ice volume changes as the glacier grows or shrinks, the continental lithosphere bends such that the total mass of the ice-sheet-lithosphere-asthenosphere column remains constant. The deflection of the lithosphere follows immediately from the evolving geometry of the ice sheet, and the ratio of the overlying fluid density (water or ice), to that of the substratum. In equilibrium, the output ice-flux of the coupled glacier-bedrock system (Q_g) equals the surface mass balance integrated over the glacier catchment and the glacier and bedrock geometry do not change.

2.1 Flow-line model

To simulate the dynamics of a coupled outlet-glacier bedrock system, we begin with a 1-D (flowline) version of the ice-sheet-bedrock model developed by Pollard and Deconto (2012). The evolution of local ice thickness at each grid node reflects the

balance of mass exchange at the surface and horizontal ice-flux divergence:

$$\frac{\partial h}{\partial t} = S - \frac{\partial \bar{u}h}{\partial x}, \tag{1}$$

where S is the local surface mass balance and $\bar{u}$ is the depth-averaged horizontal ice velocity. The velocity profiles have contributions from longitudinal stretching, shear, and basal sliding.

See table 1 for descriptions of each parameter. Response time series of glacier length, thickness and the bedrock slope are shown in figure 2 forced with the same white noise surface mass balance used in the initial example.

Bedrock elevation changes with ice and ocean loading as a combination of time-lagged asthenosphereic relaxation towards isostatic equilibrium, and modification of the applied load by the elastic lithosphere. The downward deflection w_b of the fully relaxed response is given by

$$D\nabla^4 w_b + \rho_b g w_b = q \tag{2}$$

where $D = 10^{25} N \cdot m$ is the flexural rigidity of the lithosphere, ρ_b is the bedrock density and g is gravitational acceleration. The applied load is

$$q = \rho_i g h + \rho_w g h_w - \rho_i g h_i^{eq} - \rho_w g h_w^{eq} \tag{3}$$

where h is ice thickness, h_w is ocean column thickness and h^{eq} and h_w^eq are their values in the equilibrium state. The deflection is summed over indiviual point loads of all grid cells, and assumed to be proportional to the unbalanced pressure at the top of the asthenosphere. The actual bedrock rate of change is given by:

$$\frac{\partial h_b}{\partial t} = -\frac{1}{\tau}\left(h_b - h_b^{eq} + w_b\right) \tag{4}$$

where h_b is the current bedrock elevation, h_b^{eq} is its equilibrium value and τ is the $\approx 3000yr$ asthenosphere relaxation timescale.

2.2 kinematic model

Ice-sheet mass change can be described in two stages for an idealized stable ice-sheet (Robel et al 2018; Christian et al 2020). In the first stage, accumulation falls in the interior and flows under its own weight towards the outlet glacier margins. The surface mass balance flux ($L \cdot S$) is modified by the interior flux (Q) according to the partitioning of stress accommodated by internal deformation and basal traction. The interior reservoir of the ice-sheet drains according to this interior flux until it reaches the second stage where stresses change as the glacier goes afloat giving rise to a kinematic grounding line flux Q_g, that depends nonlinearly on the grounding zone ice thickness, h_g,

$$Q_g = \Omega h_g^{\beta}. \tag{5}$$
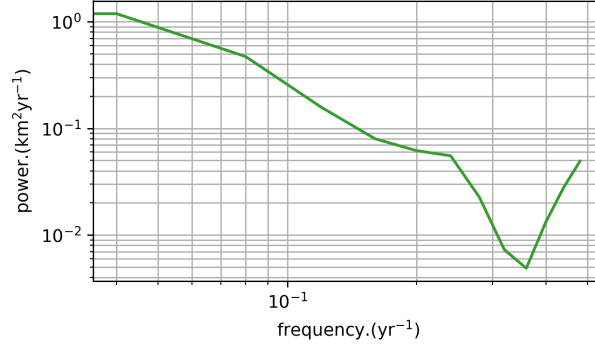
Figure 1. (a) Model schematic and response to forcing..

Two coupled equations capture the response of H, the interior thickness, and L, the glacier length, as they relax towards a
85   steady state that balances all three fluxes:

$$\frac{dH}{dt} = S - \frac{Q}{L} - \frac{H}{h_g L}(Q - Q_g) \tag{6}$$

$$\frac{dL}{dt} = \frac{1}{hg}(Q - Q_g). \tag{7}$$

Descriptions of the kinematic fluxes $(L \cdot S, Q, Q_g)$ with time series of forcing (i.e. surface mass balance, S and ocean melt rate,
Ω) form a closed system of ordinary differential equations that describe variations in glacier thickness and length. To review
90   the behavior of this coupled two-stage system and introduce the parameters that describe glacier response, we use variations
of the equilibrium two-stage ice-steam geometry described by Christian et al. (2020; Figure 1). The domain begins at an ice
divide and thus has a zero-flux boundary condition. The surface mass balance is $0.5 ma^{-1}$ ice equivalent and is assumed to be
spatially uniform across the interior. The glacier has an equilibrium length of $\approx 185 km$, a maximum thickness of $\approx 1410m$,
and a grounding line thickness of $\approx 526m$, which are generally representative of Greenland outlet glaciers and paleo-ice sheets
95   of North America. The bed elevation at the ice divide is $-100m$, and the equilibrium slope is $2m/km$.

To demonstrate the glaciological sensitivity of the filtering properties of the two stage model, we adopt two parameterizations
of the interior flux, Q, and grounding zone flux, Q_g associated with a glacier sliding over hard bedrock (form-drag friction
relation), and a glacier sliding over deformable sediment (coulomb friction relation). These two parameterizations do not
bound the behavior of glacier response (), but give some sense of glaciological parameter sensitivity to applied forcing that can
100   compare with simulations with an additional bedrock deflection stage.

Using synthetic time series of white noise ocean melt and surface mass balance anomalies with variance equal to 10% of
the equilibrium interior surface mass balance flux and equilibrium ocean flux, we force glaciers parameterized with different
flux criteria normalized to have the same equilibrium geometry and analyze their length change spectra (figure 2). In these
simulations the bedrock topography is fixed, and the response spectra can be described using spectral power laws that represent
105   the physical processes that result from nonlinear energy transfer between the applied forcing and the mechanics of sliding and
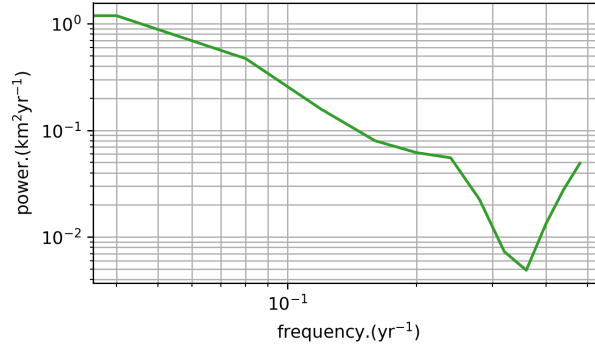
Figure 2. (a) Glacier length and thickness change for a regularized coloumb and hard-bedded outlet glacier system. (b) Power spectral density for each glacier as a function of frequency calculated via Welch's method with a window of $1/16$ the total time series (10^6 years).

ice flow. The spectra capture the ice sheet's capacity to filter different frequencies of forcing and demonstrate the glaciological sensitivity of the glacier-bedrock system to the grounding zone flux parameterization. In agreement with Schoof et al (2007) and Tsai et al (2015), the regularized coulomb friction glacier is more sensitive to ocean melt variability than the hard-bedded glacier.

110   From these grounding zone flux conditions, we see principal glaciological controls change the responsiveness of the two-stage marine ice sheet to perturbations in the surface mass balance and ocean mass balance forcing by changing the intrinsic properties of the glacier filter

Figure 2. The response function of the marine glacier forced with the same white noise variability in surface mass balance for the grounding line flux assuming different relationships between sliding speed and basal shear stress are shown in figure 2.

Symbol	Meaning
L	glacier length
H	interior thickness
b_x	bedrock slope
h_g	grounding zone thickness
Q	interior flux
Q_g	grounding zone flux
b_{x_0}	equilibrium bedrock slope
τ	response time of solid earth

Table 1. Mathematical symbols

3 A simple model for the coupled solid-earth outlet-glacier system

The simplest model for bedrock adjustment is based on the principle of local isostatic equilibrium. The lithosphere is assumed to be in floating equilibrium with the underlying heavier substrate in the asthenosphere, and the total mass of a vertical column is constant. When an ice sheet is present, the lithosphere bends downward, replacing part of the heavier material in the asthenosphere, such that the total mass of the column is constant. The deflection follows immediately from the ice geometry defined by the ice thickness H, glacier length L, and the ratio of the overburden fluid density (ice, or water) to that of the substratum. The adjustment in bedrock slope deflection is modulated by the viscous flow of the asthenosphere, which has a characteristic response time, τ. This change in bedrock slope defines the new bed geometry and grounding line position, introducing a third stage to the outlet glacier model. The new system of equations that define the glacier-bedrock system are:

$$\frac{dL}{dt} = \frac{1}{h_g(L, b_x)} \cdot (Q(L, H) - Q_g(L, b_x)), \tag{8}$$

$$\frac{dH}{dt} = S - \frac{Q_g(L, b_x)}{L} - \frac{H}{h_g(L, b_x)L} \cdot (Q(L, H) - Q_g(L, b_x)), \tag{9}$$

$$\frac{db_x}{dt} = -\frac{1}{\tau}(b_x - b_{x_0}). \tag{10}$$

3.1 Projection of variability on system eigenmodes

The outlet glacier model equations (2-4) can be linearized to understand changes in the glacier length, thickness, and bedrock slope about a local equilibrium position $\bar{L}, \bar{H}$, and $\bar{m}$. At this stable equilibrium, the interior and grounding zone fluxes balance one another and the evolution of fluctuations about the average length, thickness and slope can be written as

$$\frac{\partial}{\partial t}\mathbf{Y} = \mathbf{J}\mathbf{Y} + \mathbf{S}f(t) \tag{11}$$

$$\frac{\partial}{\partial t}\begin{bmatrix} L' \\ H' \\ b'_x \end{bmatrix} = \begin{bmatrix} A_L & A_H & A_{b_x} \\ B_L & B_H & B_{b_x} \\ C_L & C_H & C_{b_x} \end{bmatrix}\begin{bmatrix} L' \\ H' \\ b'_x \end{bmatrix} + \begin{bmatrix} \bar{h_g}^{-1} \\ \bar{L}^{-1}\left(\frac{\bar{H}}{\bar{h}_g} - 1\right) \\ 0 \end{bmatrix} Q'_g + \begin{bmatrix} 0 \\ 1 \\ 0 \end{bmatrix} S' \tag{12}$$

where $A_H, A_L, A_m, B_H, B_L, B_m, C_H, C_L,$ and C_m describe the couplings between length, thickness, and bed-slope changes (Christian et al 2020; see appendix for coefficient solutions), and Q'_g and S' describe the projection of terminus and interior climate forcing on each state variable. The coupling described by each coefficient is significantly more complex because of the additional feedback with the bedrock slope, so we substitute representative glacier geometry, rheology and sliding parameter values into the vectorized system of equations to understand the solution character empirically. The parameters used are shown in table 2.

With the addition of the third-stage wherein the bedrock slope is allowed to respond with length and thickness change, we find that the solutions for linearized glacier-bedrock model become complex. We project the vector-form equation for the

parameter	value
equilibrium length, $\bar{L}$ (km)	182
equilibrium thickness, $\bar{H}$ (m)	1412
equilibrium slope, $\bar{b}_x$ (m/km)	-2
sliding exponent, m	1/3
sliding coefficient C $(Pa \cdot m^{-1/3} s^{1/3})$	7624000
deformation exponent, n	3
seawater density, ρ_w $(kg \cdot m^{-3})$	1028
ice density, ρ_i $(kg \cdot m^{-3})$	917
bed elevation at divide, b_0 (m)	-100
β	19/3
γ	3
τ (yr)	3000

Table 2. Mathematical symbols

system on to the system eigenmodes, which can be written as simple one-dimensional linear ordinary differential equations for which we can write the green's function in the time domain, the power spectral density, and the covariance function explicitly to further understand the character of the response.

$$\frac{d}{dt}m_s = \qquad\qquad -\alpha_s m_s + \sigma_s f(t) \qquad\qquad (13)$$

$$\frac{d}{dt}m_f = \qquad\qquad -\alpha_f m_f + \sigma_s f(t) \qquad\qquad (14)$$

$$\frac{d}{dt}m_i = \qquad\qquad -\alpha_i m_i + \sigma_i f(t) \qquad\qquad (15)$$

Figures *-* demonstrate that the inclusion of isostatic adjustment significantly changes the response of marine-terminating outlet glaciers. In the next section, we examine the consequences of filtering properties of the coupled ice-sheet-bedrock system for three key questions in glaciology: How does GIA modify the committed response of marine ice-sheets to forcing? How does damping at non-resonant frequencies affect the spectra of ice volume variability preserved in proxy records?

4   Characteristic time scales

4.1   Comparison with two-stage model

Robel et al. (2018) and Christian et al. (2020) showed that the two-stage model emulates the response of different flowline models to interior surface mass-balance anomalies and grounding flux perturbations.
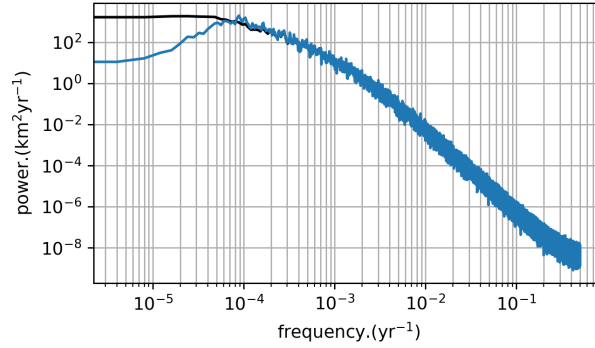
Figure 3. Model response from theoretical eigenmode decomposition. The left column is the response to precipitaion forcing ($\Delta S = -0.2$). The right column is the response to Grounding Line forcing ($\Delta Q_g = 0.2$). The projections of the eigenmodes onto the H, L are identical. The only difference comes from ($\sigma H, \sigma L$) which affects how much each type of forcing excites the fast and slow eigenmodes. In particular, we notice that Grounding line forcing excites the fast mode much more strongly than precipitation forcing does.
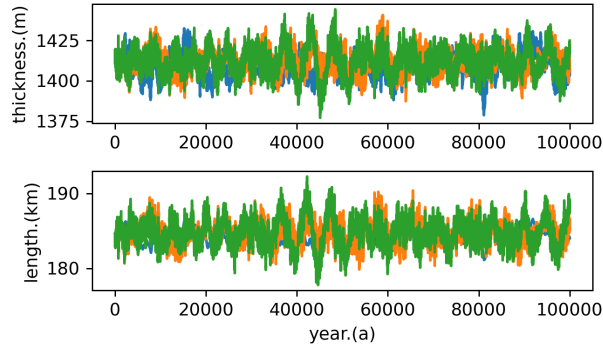
Figure 4. Time series of the glacier length and thickness variations for a simulation with the bedrock geometry fixed, and a simulation with the bedrock slope allowed to vary.

155   Figure 2 shows output from the two stage marine outlet glacier model and the model that also includes variations in bedrock slope due to GIA.

5   summary and discussion

5.1   Climate-bedrock feedback implications

Any system with a non-zero response time will lag the applied forcing. Committed change refers to the total response such a
160   system would need to undergo to attain equilibrium with the current level of forcing. In the previous sections, variability was imposed with a flat power spectra (i.e. white noise); however inertia of the climate system.

8
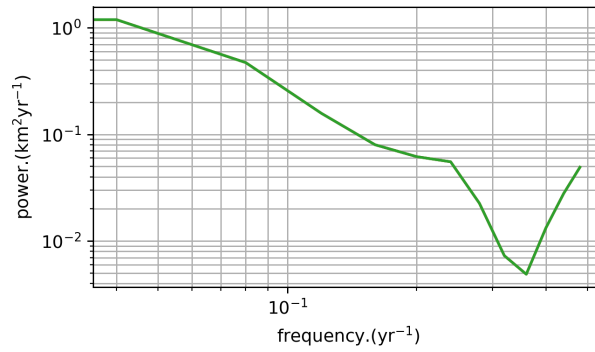
Figure 5. (a) Autocorrleation as a function of time lag. (b) Power spectral density as a function of frequency calculated via Welch's method with a window of $1/16$ the total time series (10^6 years).

5.2 sea-level

6 Conclusions

Our simple modeling demonstrates a subtle feedback between multi-milenia climate variability and the modulation of marine ice-sheet bedrock that tends to stabilize the marine ice-sheet system by damping low frequency oscillations in glacier thickness and glacier length relative to simulations that assume no bedrock response. The same feedback amplifies oscillations in glacier length at the resonant frequency of the bedrock.

Code and data availability. The code used to run the simulations included in the text is freely available at https://github.com/hoffmaao/gia2stage (last accessed April 20 2021).

9

Appendix A: Derivation of linear model

$$A_L = \frac{-\bar{H}^\alpha \bar{L}^{-1-\gamma}\gamma\nu - \bar{m}\beta\lambda\Omega((b_0 + \bar{L}\bar{m})\lambda)^{-1+\beta}}{(b_0 + \bar{L}\bar{m})\lambda} + \frac{(\bar{m}(\bar{H}^\alpha \bar{L}^-\gamma\nu + \Omega(b_0 + \bar{L}\bar{m})\lambda)^\beta)}{(b_0 + \bar{L}\bar{m})^2\lambda},$$

$$A_H = \frac{-\bar{H}^{-1+\alpha} \bar{L}^-\gamma\alpha\nu}{(b_0 + \bar{L}\bar{m})\lambda},$$

$$A_m = \frac{-((\bar{L}\beta(-(b_0 + \bar{L}\bar{m})\lambda)^{-1+\beta}\Omega)}{b_0 + \bar{L}\bar{m}} + \frac{(\bar{L}(\bar{H}^\alpha \bar{L}^-\gamma\nu - (-(b_0 + \bar{L}\bar{m})\lambda)^\beta\Omega))}{(b_0 + \bar{L}\bar{m})^2\lambda},$$

$$B_L = \frac{\bar{m}\beta\lambda(-(b_0 + \bar{L}\bar{m})\lambda)^{-1+\beta}\Omega)}{\bar{L}} + \frac{((-(b_0 + \bar{L}\bar{m})\lambda)^\beta\Omega)}{\bar{L}^2} + \frac{(\bar{H}(-\bar{H}^\alpha \bar{L}^(-1-\gamma)\gamma\nu + \bar{m}\beta\lambda(-(b_0 + \bar{L}\bar{m})\lambda)^(-1+\beta)\Omega))}{\bar{L}(b_0 + \bar{L}\bar{m})\lambda}$$

$$- \frac{(\bar{H}\bar{m}(\bar{H}^\alpha \bar{L}^-\gamma\nu - (-(b_0 + \bar{L}\bar{m})\lambda)^\beta\Omega))}{\bar{L}(b_0 + \bar{L}\bar{m})^2\lambda} - \frac{(\bar{H}(\bar{H}^\alpha \bar{L}^-\gamma\nu - (-(b_0 + \bar{L}\bar{m})\lambda)^\beta]\Omega))}{\bar{L}^2(b_0 + \bar{L}\bar{m})\lambda},$$

$$B_H = \frac{\bar{H}^\alpha \bar{L}^(-1-\gamma)\alpha\nu}{(b_0 + \bar{L}\bar{m})\lambda} + \frac{\bar{H}^\alpha \bar{L}^-\gamma\nu - (-(b_0 + \bar{L}\bar{m})\lambda)^\beta\Omega}{\bar{L}(b_0 + \bar{L}\bar{m})\lambda},$$

$$B_m = \frac{\bar{H}\beta(-(b_0 + \bar{L}\bar{m})\lambda)^{-1+\beta}\Omega}{b_0 + \bar{L}\bar{m}} + \beta\lambda(-(b_0 + \bar{L}\bar{m})\lambda)^{-1+\beta}\Omega - \frac{\bar{H}(\bar{H}^\alpha \bar{L}^-\gamma\nu - (-(b_0 + \bar{L}\bar{m})\lambda)^\beta\Omega)}{(b_0 + \bar{L}\bar{m})^2\lambda},$$

$$C_L = -\frac{-\frac{1}{3}\bar{L}\bar{m}\kappa - \frac{1}{3}(-b_0 + 2\bar{H} + \bar{L}\bar{m})\kappa}{\tau},$$

$$C_H = \frac{2\bar{L}\kappa}{3\tau},$$

$$C_m = -\frac{1 - \frac{(\bar{L}^2\kappa)}{3}}{\tau}.$$

A1

References

REFERENCE 1

REFERENCE 2